

## Simulation of a “Well Tempered” SOI MOSFET using an Enhanced Hydrodynamic Transport Model

M. Gritsch, H. Kosina, T. Grasser, and S. Selberherr

Institute for Microelectronics, TU Vienna  
Gusshausstrasse 27–29, A-1040 Vienna, Austria  
Email: Gritsch@iue.tuwien.ac.at

**Abstract** – Anomalous output characteristics are observed in hydrodynamic simulations of partially depleted SOI MOSFETs. The effect that the drain current reaches a maximum and then decreases is peculiar to the hydrodynamic transport model. It is not observed in drift-diffusion simulations and its occurrence in measurements is questionable. An explanation of the cause of this effect is given, and a solution is proposed by modifying the hydrodynamic transport model. Successful simulations of different SOI Devices including a “Well Tempered” SOI MOSFET are presented.

### I. INTRODUCTION

Using the standard hydrodynamic (HD) transport model for simulation of partially depleted SOI MOSFETs, an anomalous decrease of the drain current with increasing drain-source voltage has been observed (Fig. 1).

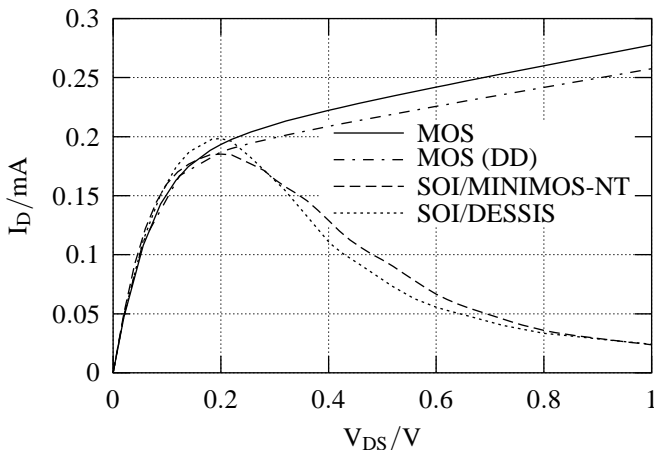


Figure 1: Output characteristics obtained by standard DD and HD simulations; verified by using two different device simulators.

The anomalous effect has been reproduced using the two device simulators MINIMOS-NT [1] and DESSIS [2], and can be explained by an enhanced diffusion of channel hot carriers into the floating body [3] [4]. It is believed that this decrease in drain current is an artifact because experimental data do not show this effect, nor can it be observed when using the drift-diffusion (DD) transport model. One exception is given

in [5], where a weak decrease of the measured drain current of a p-MOS SOI device is reported.

However, applicability of the HD model to the ever down-scaled devices is desirable, because in contrast to the DD model it takes non-local effects into account. Empirical measures provided by DESSIS, such as weighting heat flow and thermal diffusion, have only little influence on the current drop. We present a revision of the HD model which enables proper simulation of SOI MOSFETs.

### II. CAUSE OF THE EFFECT

The main difference between the HD and the DD transport model is given by the energy balance equation. The benefit of the increased computational effort of solving an additional equation is that the carrier temperature can differ from the lattice temperature. Since the diffusion of the carriers is proportional to their temperature, the diffusion can be significantly higher with the HD transport model.

When simulating SOI MOSFETs this increased diffusion has a strong impact on the body potential, because the hot electrons of the pinch-off region have enough energy to overcome the energy barrier towards the floating body region and thus enter into the sea of holes. Some of these electrons in the floating body are collected by the drain-body and source-body junctions, but most recombine. The holes removed by recombination cause the body potential to drop. A steady state is obtained when the body potential reaches a value which biases the junctions enough in reverse direction so that thermal generation of holes in the junctions can compensate this recombination process. The decrease in the output characteristics is directly connected to the drop of the body potential via the body-effect.

### III. WEIGHT FACTORS

Our first attempt to avoid the anomalous current decrease was to tune the empirical weight factors of thermal diffusion and heat flow, as provided by the HD model of DESSIS. Within this parameter space only minor improvements in the IV characteristics were possible. Therefore, our investigations continued with more physically motivated modifications using MINIMOS-NT.

#### IV. MODIFICATIONS

In Monte-Carlo (MC) simulations the spreading of hot carriers away from the interface is much less pronounced than in HD simulations (Fig. 6). If we assume that the BOLTZMANN equation does not predict the hot carrier spreading, and if the HD equations derived from the BOLTZMANN equation do so, the problem must be introduced by the assumptions made in the derivation of the HD model. Relevant in this regard is the approximation of tensor quantities by scalars and the closure of the hierarchy of moment equations.

In order to capture more realistically the phenomenon of hot carrier diffusion we derived a HD equation set from the BOLTZMANN equation permitting an anisotropic temperature and a non-MAXWELLIan distribution function:

$$J_{n,\xi} = \mu_n (k_B \nabla_\xi (n T_{\xi\xi}) + q E_\xi n) \quad (1)$$

$$S_{n,\xi} = -\frac{5}{2} \frac{k_B}{q} \mu_S \left( k_B \nabla_\xi (n \beta_n T_{\xi\xi} \Theta) + q E_\xi n \Theta \right) \quad (2)$$

$$\text{with } \nabla_\xi = \frac{\partial}{\partial \xi} \quad \text{and} \quad \Theta = \frac{3T_n + 2T_{\xi\xi}}{5} \quad (3)$$

$T_{\xi\xi}$  denotes the diagonal component of the temperature tensor for direction  $\vec{e}_\xi$ . Off-diagonal components are neglected.  $\beta_n$  is the normalized moment of fourth order.

By setting  $T_{\xi\xi} = T_n$  and  $\beta_n = 1$  the conventional HD model is obtained. The solution variable is still the carrier temperature  $T_n$ , whereas the tensor components and  $\beta_n$  are modeled empirically as functions of  $T_n$ . First empirical modeling of  $T_{\xi\xi}$  was performed by distinguishing between directions parallel and normal to the current density:

$$T_{\xi\xi} = T_{xx} \cos^2 \varphi + T_{yy} \sin^2 \varphi, \quad T_{xx} = \gamma_x T_n, \quad T_{yy} = \gamma_y T_n \quad (4)$$

$$\gamma_v(T_n) = \gamma_{0v} + (1 - \gamma_{0v}) \exp\left(-\left(\frac{T_n - T_L}{T_{\text{ref},\gamma}}\right)^2\right), \quad v = x, y \quad (5)$$

The anisotropy functions  $\gamma_v(T_n)$  give 1 for  $T_n = T_L$  and an asymptotic value  $\gamma_{0v}$  for large  $T_n$ , that only for sufficiently hot carriers the distribution becomes anisotropic, whereas the equilibrium distribution stays isotropic (Fig. 2). With respect to numerical stability the transition should not be too steep.  $T_{\text{ref},\gamma} = 600 \text{ K}$  appeared to be appropriate.

Another effect observed in MC simulations is that in most parts of the channel the high energy tail is less populated than that of a MAXWELLIan distribution, which gives  $\beta_n < 1$  (Fig. 3).

$$\beta_n(T_n) = \beta_0 + (1 - \beta_0) \exp\left(-\left(\frac{T_n - T_L}{T_{\text{ref},\beta}}\right)^2\right) \quad (6)$$

The functional form of  $\beta_n(T_n)$  is identical to the one of the anisotropy function  $\gamma_v(T_n)$  (cf. eqn. (5)). Again, this expression ensures that only for sufficiently large  $T_n$  the distribution deviates from the MAXWELLIan shape.

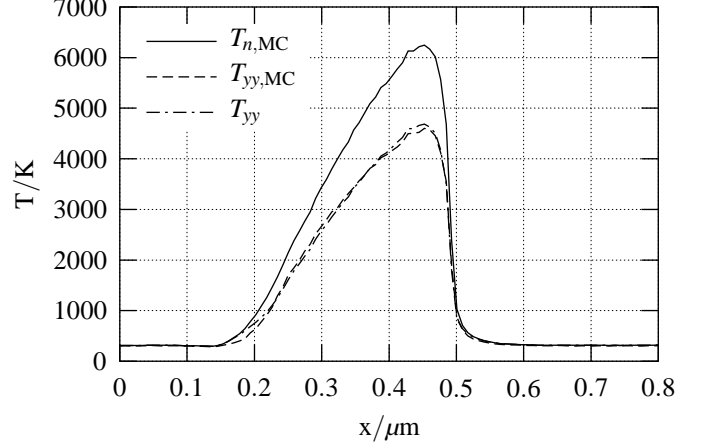


Figure 2: MC simulation of an *nin*-structure showing the *x*-component of the temperature compared to the mean temperature  $T_{n,MC}$ . The analytical  $T_{yy}$  uses  $\gamma_{0y} = 0.75$ .

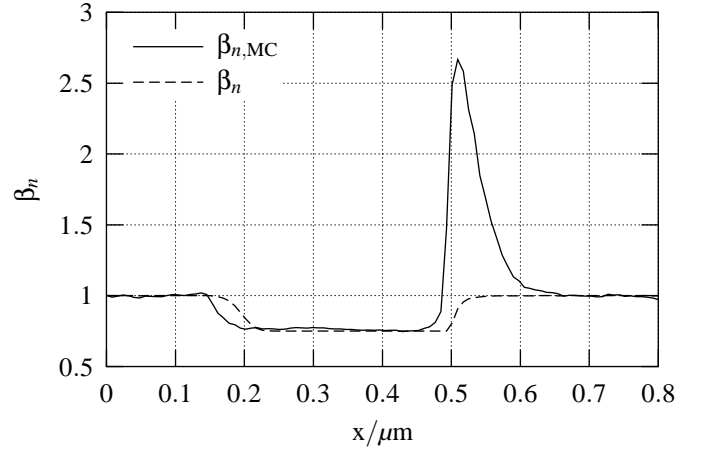


Figure 3: MC simulation of a *nin*-structure showing the normalized moment of fourth order  $\beta_{n,MC}$  compared to the analytical  $\beta_n$  with  $\beta_0 = 0.75$ .

#### V. RESULTS

The modified flux equations have been implemented in MINIMOS-NT using a straight forward extension of the Scharfetter-Gummel discretization scheme. Numerical stability does not degrade compared to standard HD simulations. Parameter values were estimated from MC results for one-dimensional test structures.

As a first example simulations were performed on a device with an assumed effective gate-length of 130 nm, a gate-oxide thickness of 3 nm, and a silicon-film thickness of 200 nm. With a p-doping of  $N_A = 7.5 \cdot 10^{17} \text{ cm}^{-3}$  the device is partially depleted. The Gaussian shaped n-doping under the electrodes has a maximum of  $N_D = 6 \cdot 10^{20} \text{ cm}^{-3}$ .

Fig. 2 indicates that  $\gamma_{0y} = 0.75$  is a realistic value for the anisotropy parameter. Fig. 4 shows the influence of  $\gamma_{0y}$  on the output characteristics. By accounting for a reduced ver-

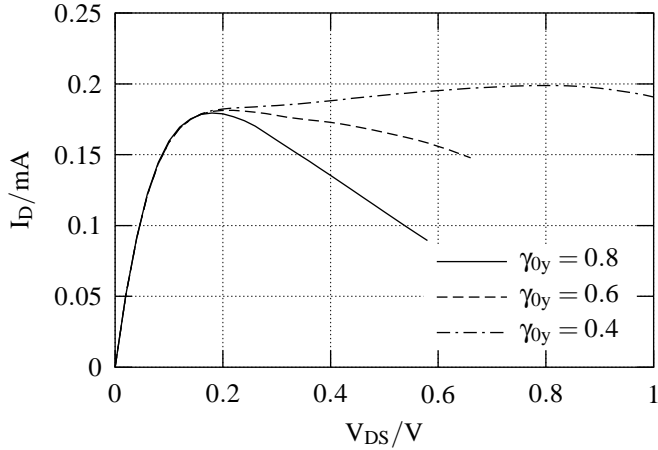


Figure 4: Output characteristics of the SOI obtained by anisotropic HD simulations without closure modification ( $\beta_0 = 1$ ).

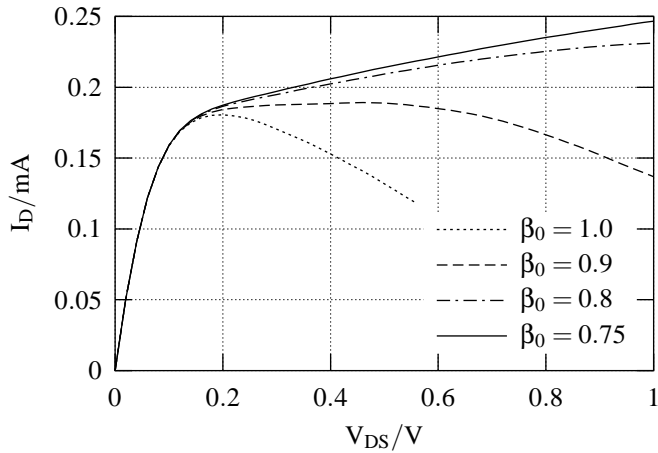


Figure 5: Output characteristics of an SOI-MOSFET with analytical doping profile assuming an anisotropic temperature ( $\gamma_{0y} = 0.75$ ) and a modified closure relation.  $V_{GS} = 1V$ .

tical temperature it is possible to reduce the spurious current decrease, but only to a certain degree and by assuming a fairly large anisotropy. MC simulations yield values close to  $\beta_0 = 0.75$  for the non-MAXWELLian parameter in the channel region (Fig. 3). This parameter shows only a weak dependence on doping and applied voltage.

By combining the modifications for an anisotropic temperature and a non-MAXWELLian closure relation the artificial current decrease gets eliminated (Fig. 5). Parameter values roughly estimated from MC simulations can be used, e.g.  $\gamma_{0y} = 0.75$  and  $\beta_0 = 0.75$ . In the parameter range where the current drop is eliminated the output characteristics are found to be rather insensitive to the parameter values.

Comparing the electron concentration in a MOSFET at a vertical cut located in the middle between source and drain obtained by using DD-, HD-, MC-, and our modified HD model,

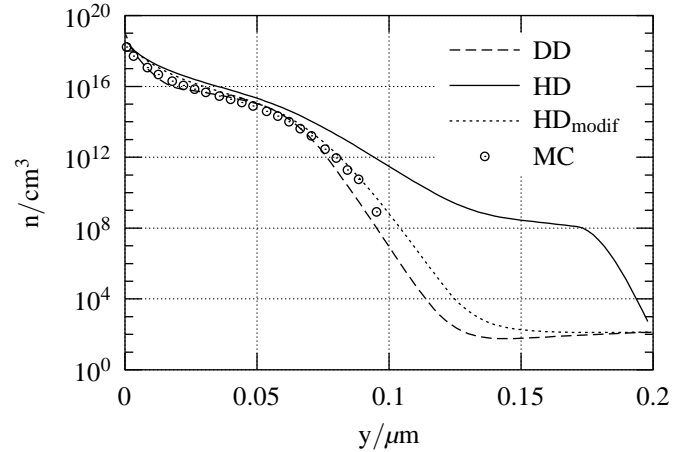


Figure 6: Electron concentration in a MOSFET at a vertical cut located in the middle between source and drain obtained by simulations using DD-, HD-, MC-, and our modified HD model.

good agreement between our model and MC data is obtained (Fig. 6). This confirms that the correction of the SOI output characteristics obtained by the modified model is based on a corrected behavior of the electron distribution in the bulk.

To verify the modified hydrodynamic transport model, a second device has been investigated. Basically this SOI has been modeled after the 90 nm “Well-Tempered” MOSFET [6] using the doping profiles available online, including the SSR channel doping and source/drain halo. To achieve a partially depleted device a substrate doping of  $N_A = 7.5 \cdot 10^{17} \text{ cm}^{-3}$  has been assumed, and the substrate thickness has been limited to 200 nm.

The difference in the electron concentration is shown in Fig. 7 and Fig. 8. In the case of the standard HD model, the spreading of the hot electrons is much more pronounced than with the modified one.

By using the standard HD transport model the drop in the drain current is also present in this device ( $\beta_0 = 1.0, \gamma_{0y} = 1.0$  in Fig. 9). Applying the modified model using the same parameters as before the output characteristics obtain their normal shape. The different order of magnitude of the drain currents seen with Device 1 and Device 2 mainly stems from the rather high threshold voltage of Device 1.

By looking at the potential in the device at a vertical cut located in the middle between source and drain (Fig. 10), the difference between the standard HD model ( $\beta_0 = 1.0$ ) and the modified one ( $\beta_0 = 0.75$ ) is also clearly visible.

It appeared that in contrast to MOS devices the grid in the floating body region plays a crucial role with regard to the stability of the simulation and the quality of the result because the drain current is very sensitive to the location of the potential drop in the floating region.

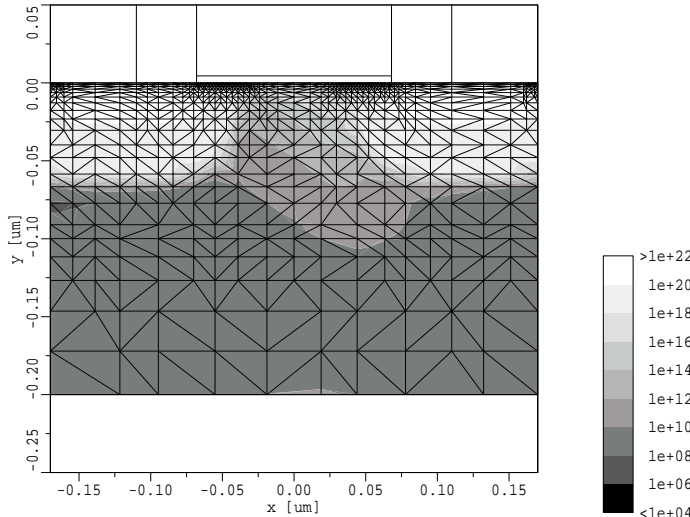


Figure 7: Electron concentration in the well tempered SOI obtained by a standard HD simulation.

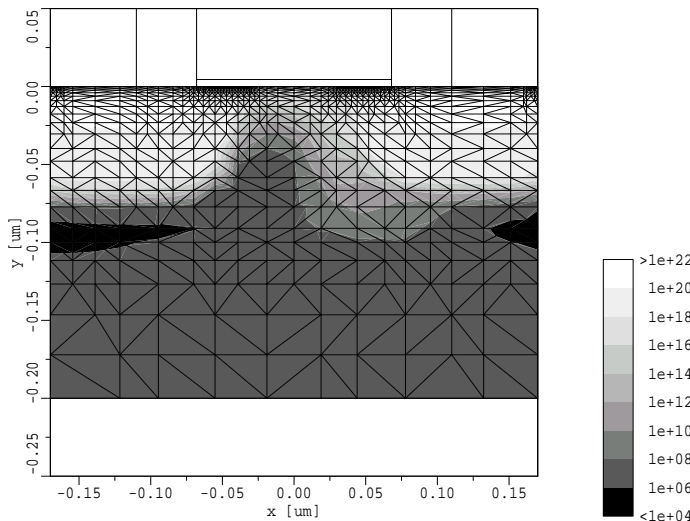


Figure 8: Electron concentration in the well tempered SOI obtained by a modified HD simulation ( $\beta_0 = 0.75$ ).

## VI. CONCLUSION

Standard HD simulations of SOI MOSFET give anomalous output characteristics. To solve this problem, an improved HD transport model has been developed. By including two distinct modifications, namely an anisotropic carrier temperature and a modified closure relation, the spurious diffusion of hot electrons in the vertical direction has been sufficiently reduced. The improved hydrodynamic transport model has successfully been used to simulate different SOI devices.

## ACKNOWLEDGMENT

This work has been supported by the *Christian Doppler Gesellschaft*, Vienna, Austria.

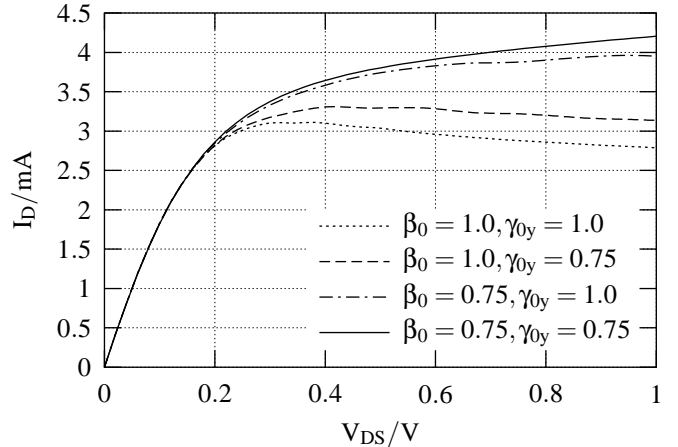


Figure 9: Output characteristics of the “Well-Tempered” SOI.  $V_{GS} = 1$  V.

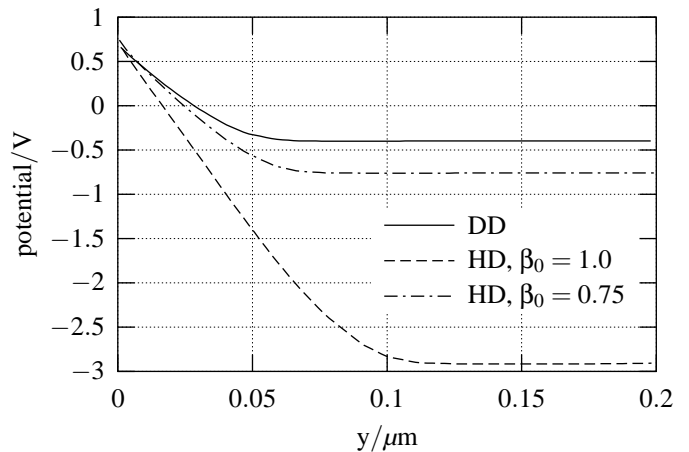


Figure 10: Vertical potential distribution in the well tempered SOI at a vertical cut located in the middle between source and drain.

## REFERENCES

- [1] T. Simlinger, H. Brech, T. Grave, and S. Selberherr, *IEEE Trans. Electron Devices* **44**, 700 (1997).
- [2] DESSIS-ISE Users Manual, Release, (6).
- [3] M. Gritsch, H. Kosina, T. Grasser, and S. Selberherr, *Solid-State Electron.* **45**, 621 (2001).
- [4] M. Gritsch, H. Kosina, T. Grasser, and S. Selberherr, in *Silicon-On-Insulator Technology and Devices X* (Washington DC, USA, 2001), pp. 181–186.
- [5] J. Egley, B. Polsky, B. Min, E. Lyumkis, O. Penzin, and M. Foisy, in *Simulation of Semiconductor Processes and Devices* (Seattle, Washington, USA, 2000), pp. 241–244.
- [6] D. Antoniadis, I. Djomehri, K. Jackson, and S. Miller, “Well-Tempered” Bulk-Si NMOSFET Device Home Page, <http://www-mtl.mit.edu/Well/>, 2001.